Science and Technology Indonesia
e-ISSN:2580-4391 *p*-ISSN:2580-4405
Vol. 11, No. 1, January 2026

Research Paper

Cogon Grass Mesoporous Silica Nanoparticles Loaded with *Uncaria gambir* Extract and Photosensitizer for Photothermal Induced Anti-MRSA Activity: Formula Optimization and In Silico Exploration

Mardiyanto[1], Tia Sabrina[2], M. Faris Alhafizh[1], Natacha Brigida Kota[1], Sheza Inayah Ramadhona[1], Novella Valenia[1], M. Ammar Amrullah[1], Daghfal Rafataqwa Zulda[1], R.D. Nindi Marrisca[1,3], Sutan Satya Alisyahbana[1], Ade Fadilah[1], Aisyah Pratiwi[1], Najma Annuria Fithri[1,3*]

[1]*Department of Pharmaceutical Technology, Pharmacy Major, Faculty of Mathematics and Natural Sciences, Sriwijaya University, Ogan Ilir, 30862, Indonesia*
[2]*Department of Microbiology, Faculty of Medicine, Sriwijaya University, Palembang, 30139, Indonesia*
[3]*Research Centre of Drug Delivery and Nanomaterial Fabrication, Pharmacy Major, Faculty of Mathematics and Natural Sciences, Sriwijaya University, Ogan Ilir, 30862, Indonesia*
*__Corresponding author__: najma.fithri@mipa.unsri.ac.id

Abstract
In recent years antimicrobial resistance (AMR) has grown to become a massive concern for the global community due to their lack of successful prevention and low recovery rates. One of methods with high efficiency in reducing AMR is photodynamic and photothermal therapy (PDPT), due to their independency from chemical mechanism of antimicrobial efficacy. Mesoporous silica nanoparticle (MSN) is an excellent carrier for potential alternative for AMR including photosensitizers and natural based active ingredients. Herein, we explored the use of various sources as silica precursors as well as optimization based on method of fabrication and coating agent to stabilize and load the active ingredients. We additionally incorporated *Uncaria gambir* extract and phycocyanin to increase MSN antimicrobial effect and photosensitizing ability. Cogon grass-based MSN (CG-MSN) has yet to be explored extensively and in this research, we compared their characteristics to a more established precursors such as tetraethyl orthosilicate (TEOS) and sodium silicate. Based on the results obtained, cogon grass-based precursors produced the highest yield, with entrapment efficiency of *Uncaria gambir* and phycocyanin as high as 98%. Furthermore, CG-MSN produced one of the highest photothermal increase and adsorption rate comparable to that of TEOS. From in silico exploration *Uncaria gambir* contained Gambiriin and Roxburghin as two of the most active phytoconstituents that influenced its antimicrobial activity. Based on this research we were able to synthesize a new precursor of silica from natural based product, cogon grass, and incorporate it as carrier for phytocompounds in the management of AMR.

Keywords
Antimicrobial Resistance, Cogon Grass Silica, Mesoporous Silica, Photodynamic and Photothermal Therapy, *Uncaria gambir* Extract

Received: 3 September 2025, Accepted: 1 December 2025
https://doi.org/10.26554/sti.2026.11.1.311-322

1. INTRODUCTION

Antimicrobial resistance (AMR) has been an emergency case in the worldwide health industry and prevents from maximizing the success of infection treatment (Ho et al., 2025). This phenomenon occurs when bacteria lose its ability to receive total treatment from antibiotics, thus threatening the effectiveness of conventional treatment and will enhance the risk of infection in the immediate future (Ahmed et al., 2024). According to a 2019 study by Global Burden of Disease, approximately 50% of antimicrobials-resistant bacterial pathogens cases were associated with *Staphylococcus aureus*, killing mostly humans older than age of 15 in 135 countries. GBD also estimated 4.71 million deaths caused by bacterial AMR in 2021 (Ikuta et al., 2022; Naghavi et al., 2024). Emergence of AMR is commonly initiated by a failed traditional one-drug one-enzyme pathway as bacteria pathogens keep evolving to digress from conventional drug mechanisms, for example Methicillin-resistant S. aureus (MRSA) (Singha et al., 2024). Traditional antibiotic treatment that targets intracellular bacterial infections faces multiple obstacles, which with drug delivery system hopes to enhance cell membrane permeability and antibiotic retention time (Liu et al., 2025).

Phototherapy has emerged as a promising non-invasive strategy in biomedical applications, particularly through photodynamic therapy and photothermal therapy (PDPT). In photodynamic therapy, the process usually involves three essential components: a specific wavelength of light, a photosensitizer

(PS), and molecular oxygen, which collectively interact to produce cytotoxic reactive oxygen species (ROS) that lead to cellular damage (Fithri et al., 2025). In contrast, photothermal therapy employs light-typically in the near-infrared (NIR) region-to elevate local tissue temperature, inducing cell death through protein denaturation and disruption of cell membranes (Azzahra et al., 2025; Fithri et al., 2025). This thermal effect is achieved by applying relatively high light intensities to reach uncoagulated conditions (43-55 °C) or coagulative (55-100 °C) temperature ranges (Overchuk et al., 2023). The efficacy of PDPT depends significantly on the choice of photosensitizer. While many studies have explored synthetic chemical compounds, increasing attention has been directed toward natural photosensitizers due to their biocompatibility and lower toxicity (Cieplik et al., 2018). Phycocyanin, a blue-colored pigment derived from *Spirulina platensis*, is one such natural photosensitizer. It exhibits efficient light absorption, particularly in the NIR region, and demonstrates minimal toxicity toward healthy cells, making it a suitable candidate for phototherapy applications (Abbasianfar et al., 2024).

Recent developments in NDDS have focused on stimuli-responsive systems, which are engineered to release their payload in response to internal conditions (e.g., acidic pH in inflamed tissues or elevated enzyme levels) or external triggers (e.g., heat, light, or magnetic fields). These systems allow for precise spatiotemporal control over drug release. Moreover, NDDS are being explored not only for intravenous applications but also for oral, transdermal, and mucosal routes, offering improved patient compliance and administration flexibility (Vallet-Regí et al., 2022; Zhang et al., 2016). Despite their promising preclinical performance, the clinical translation of NDDS faces several challenges, including formulation stability, long-term safety concerns, regulatory compliance, and large-scale manufacturing (Varala et al., 2023; Zhang et al., 2016). Ongoing research continues to optimize the design, functionality, and biocompatibility of NDDS to fully realize their potential in modern therapeutics.

Mesoporous silica (MSN) has attracted substantial interest in recent years owing to its distinctive physicochemical properties, including large specific surface area, tunable pore size (2-50 nm), high thermal and mechanical stability, and ease of surface functionalization (Narayan et al., 2018; Han et al., 2024). According to the International Union of Pure and Applied Chemistry (IUPAC), mesoporous materials are defined as solids possessing pore diameters between 2 and 50 nm with an ordered porous architecture (Narayan et al., 2018). These properties make MS materials highly versatile for applications in drug delivery, catalysis, adsorption, sensing, and environmental remediation (Krishnan et al., 2022).

The synthesis of MSN typically follows the sol-gel route, where silica precursors undergo hydrolysis and condensation in the presence of structure-directing agents such as cetyltrimethylammonium bromide (CTAB) or Pluronic block copolymers. Among various silica sources, tetraethyl orthosilicate (TEOS) is the most widely employed due to its high reactivity and ability to form uniform structures such as MCM-41 and SBA-15V (Narayan et al., 2018; Putz et al., 2015). TEOS-derived MSNs often show excellent morphological control, narrow particle size distribution, and well-ordered pore arrangement, making them suitable for biomedical applications including drug and gene delivery systems (Han et al., 2024).

Despite its advantages, TEOS is relatively expensive and not environmentally friendly, prompting researchers to explore alternative, more sustainable silica sources. One such alternative is sodium silicate (Na_2SiO_3), also known as water glass, which is more economical and readily available. Sodium silicate has been successfully utilized to synthesize SBA-15 with well-ordered 2D hexagonal pore symmetry, high surface area (up to ~800 m^2/g), and good thermal stability. In addition, the pore characteristics of SBA-15 synthesized from sodium silicate can be tuned by adjusting parameters such as aging time, calcination temperature, and precursor concentration (Rahmat et al., 2016).

In recent years, biogenic silica sources have gained traction as part of green chemistry approaches. Agricultural biomass such as cogon grass (*Imperata cylindrica*) is rich in silica content and represents a renewable, low-cost, and eco-friendly alternative (Han et al., 2024; Krishnan et al., 2022). The green synthesis of mesoporous silica from cogon grass typically involves calcination of plant ash to extract silica, followed by sol-gel processing. This approach not only re-utilizes agricultural waste but also minimizes the use of hazardous chemicals and energy, aligning with sustainable development goals (Krishnan et al., 2022). MSN derived from cogon grass has been reported to possess comparable properties to those synthesized from TEOS or sodium silicate, including ordered microporosity, high surface area, and biocompatibility-highlighting its potential in biomedical and environmental applications (Han et al., 2024; Krishnan et al., 2022).

The primary purpose of applying polymer coatings to nanoparticle surfaces is to enhance their performance in biological systems. Coatings can prevent aggregation, prolong systemic circulation, and reduce premature degradation or opsonization by the immune system. Furthermore, polymer layers allow the controlled release of active agents, including antibiotics, and can be engineered to respond to specific environmental stimuli, such as pH or enzymes, making them particularly suitable for site-specific drug delivery applications. The advantages of polymer coatings are manifold. They provide a protective barrier that improves nanoparticle dispersion stability and enhances bioavailability. Coated systems often exhibit improved pharmacokinetics and biodistribution, reducing off-target effects and increasing therapeutic efficacy (Mardiyanto et al., 2020). In antibacterial applications, such as for methicillin-resistant *Staphylococcus aureus* (MRSA), polymer coatings can be used to modulate the release of encapsulated antibiotics or to introduce additional antibacterial functionalities through embedded or covalently bound agents.

This research aims to find the best formulation of MSNs with three factors: (1) silica precursor (cogon grass, tetraethyl

orthosilicate (TEOS), or sodium silicate) (2) fabrication method (furnace calcination or reflux method), (3) coating agent (chitosan or gelatin). In this study, MSNs were targeted to show distinctive temperature increase from laser exposure, excellent entrapment of drugs, high methylene blue adsorption, and noticeable antibacterial activity. Therefore, this research was performed with design of experiment approach to optimize MSNs as alternative treatment for bacterial AMR.

2. EXPERIMENTAL SECTION

2.1 Materials

Materials used in this research including solvents were pro analysis and pharmaceutical grade. Uncaria gambier extract were obtained at Babat Toman Village, Musi Banyuasin, Indonesia, meanwhile cogon grass was sourced locally from surrounding areas in Indralaya, Ogan Ilir. Analytical grade sodium silicate, tetraethyl orthosilicate, CTAB were purchased from Sigma-Aldrich, Jakarta. Solvents and reagents used within this study including hydrochloric acid, ammonium hydroxide and sodium hydroxide were purchased in bulk from PT Bratachem Indonesia.

2.2 Methods

2.2.1 Preparation of Cogon Grass as Silica Precursor

Preparation of cogon grass as a silica precursor was conducted following the procedure of Dorairaj et al. with modification. The cogon grass was initially rinsed with water to remove surface contaminants and then dried in an oven at 100 °C for 24 hours. It was then subjected to acid treatment by boiling in a 1 M hydrochloric acid solution at 80 °C for 2 hours. Afterward, the sample was thoroughly washed several times with distilled water to eliminate residual acid and impurities, followed by overnight drying at 90 °C. Prior to calcination, the dried material was ground to achieve uniform combustion. The calcination process was carried out at a modified condition of 500 °C for 21 hours in a furnace to ensure complete thermal decomposition and silica extraction (Dorairaj et al., 2022). Ten grams of cogon grass ash was refluxed with a 3.5 M sodium hydroxide solution at 80 °C for five hours under continuous vigorous stirring. The resulting mixture was filtered using Whatman filter paper (0.45 μm) to obtain a clear and viscous solution. This filtrate was designated as the cogon grass silicate stock solution (Usgodaarachchi et al., 2021).

2.2.2 Design of Experiment

Optimization of the formulation was carried out using Design Expert Version 13 software employing the Optimal Custom Design method to evaluate the effects of three categorical factors on seven functional responses. The three investigated factors were: (1) the type of silica precursor-TEOS, sodium silicate, and natural silica derived from *Imperata cylindrica* (cogon grass); (2) the mesoporous silica synthesis process-calcination and reflux; and (3) the coating agent-chitosan or gelatin. The experimental design was structured using block 1 with four replications to ensure statistical robustness and reproducibility. The seven measured responses included: photothermal increase using 450 nm laser, entrapment efficiency (%EE) of quercetin and phycocyanin as well as adsorption rate. This experimental approach aimed to identify the optimal combination of synthesis parameters that maximize functional performance, while also elucidating potential interactions among precursor type, synthesis method, and coating agent in the development of an effective mesoporous silica-based delivery system. The condition set within this research can be seen in Figure 1.

2.2.3 Synthesis of MSNs from Cogon Grass Precursor

The synthesis of MSNs using followed a previously documented methodology with minor modification using the sol-gel method (Usgodaarachchi et al., 2021). A 2.0 wt% CTAB solution was first prepared by dissolving CTAB in a 1:1 (v/v) mixture of deionized water and 2-propanol under constant stirring. Subsequently, precursor solution was added dropwise into the CTAB solution while continuously stirring for 30 minutes to form a homogeneous mixture. The hydrolysis and condensation of precursors were initiated by slowly adding 7.5 mL 0.5 M sulfuric acid at 60 °C and homogenized for 1 hour. The resulting gel was aged at room temperature for 12 hours to allow complete formation of the silica network. The aged silica gel was then washed thoroughly with DIW to remove any remaining sulfate anions. The purified gel was dried with two different methods. First method was calcined at 500 °C for 4 hours and the second method was refluxed for 24 hours at 80 °C to remove the template and obtain the final MSNs.

2.2.4 Synthesis of MSNs from TEOS Precursor

The synthesis of MSNs using TEOS precursor followed a previously documented methodology with minor modification using the sol-gel method (Krishnan et al., 2022). A total of 4 mL ethanol and 2 mL ammonia solution were mixed into 100 mL DIW. Then, 1 g of CTAB was added to the solution. The solution was stirred at 400 rpm at room temperature for 15 minutes until the CTAB dissolved completely. After CTAB dissolved, 2.5 mL of TEOS was added dropwise. The color of the solution slowly turned cloudy (milky) within 10 minutes. The solution was further stirred for 4 hours at room temperature. The solution was finally centrifuged and washed twice using 35% ethanol:water, and the gels obtained were dried overnight inside the oven at 60 °C. The MSNs were obtained after calcination at 500 °C for 4 to 6 hours.

2.2.5 Synthesis of MSNs from Sodium Silicate Precursor

The synthesis of MSNs using followed a previously documented methodology with minor modification using the sol-gel method (Usgodaarachchi et al., 2021). A 2.0 wt% CTAB solution was first prepared by dissolving CTAB in a 1:1 (v/v) mixture of deionized water and 2-propanol under constant stirring. Subsequently, sodium silicate solution was added dropwise into the CTAB solution while continuously stirring for 30 minutes to

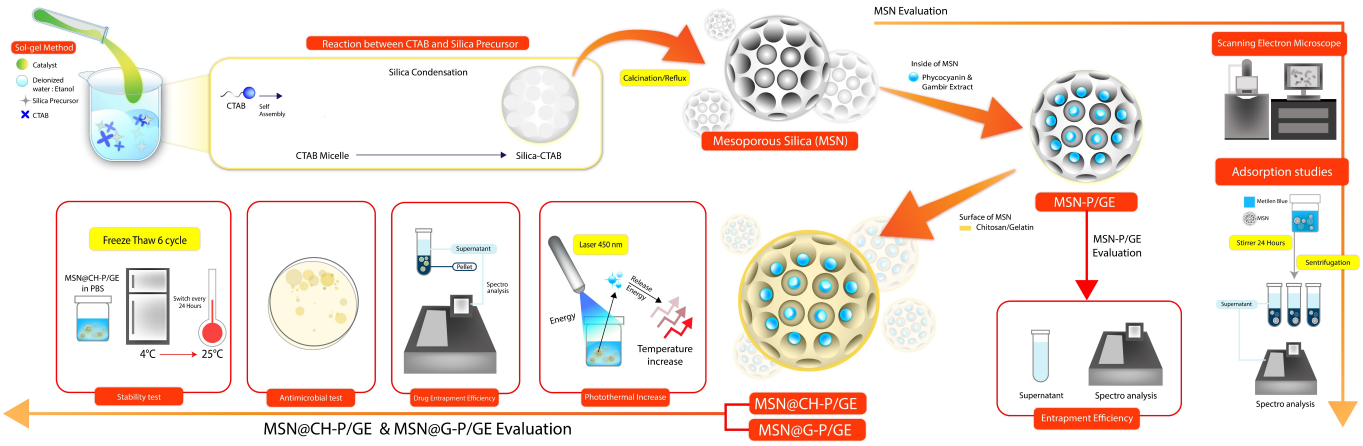

Figure 1. General Scheme of Research Conducted within This Study: Optimized Results were Evaluated for Antimicrobial Activity with and without Laser Irradiation

form a homogeneous mixture. The hydrolysis and condensation of silicate precursors were initiated by slowly adding 7.5 mL 0.5 M sulfuric acid at 60 °C and homogenized for 1 hour. The resulting gel was aged at room temperature for 12 hours to allow complete formation of the silica network. The aged silica gel was then washed thoroughly with DIW to remove any remaining sulfate anions. The purified gel was dried with two different methods. First method was calcined at 500 °C for 4 hours and the second method was refluxed for 24 hours at 80 °C to remove the template and obtain the final MSNs.

2.2.6 Phycocyanine and *Uncaria gambir* Extract Loading of MSNs (MSNs-P/GE)

Two hundred mg of MSNs were dispersed in 20 mL of DI water and sonicated for 1 hour to achieve a uniform suspension. Subsequently, 2 mL of *Uncaria gambir* extract solution and 20 mg of phycocyanin were added to the suspension and stirred continuously for 24 hours to allow the reaction to occur (Zhu et al., 2022).

2.2.7 Gelatin and Chitosan Coating of MSNs (MSN@G-P/GE) (MSN@CH-P/GE)

The coating was performed with 2 different coating. For chitosan, 0.6 gr 0.6% w/v chitosan in acetic acid aqueous (10% v/v) solution was prepared and the pH was adjusted to 6.0. Then 0.1 g MSNs was added and stirred for 48 h. After 48 h, centrifuge the mixture and washed with DI water twice. Dried the sample in oven for 24 h at 100 °C. Then the resulting products were obtained (Chen and Zhu, 2012). For gelatin coated MSNs, 0.6 gram of gelatin was dissolved in 100 mL aquadest, 0.6% (w/v) and the pH was adjusted to 6.0. 0.1 gr of MSNs was addend into solution and stirred for 48 h. After 48 h, centrifuge the mixture and washed with DIW twice. Dried the sample in oven for 24 h at 100 °C. The resulting products were obtained (Nasab et al., 2018).

2.2.8 SEM and XRD Analysis

For morphological and evaluation of characteristics from the optimised MSN, SEM and XRD analysis were performed. Samples were taken and prepared according to the protocol used for each evaluation. Gold coating was performed for SEM analysis for elemental mapping.

2.2.9 Adsorption Studies

The adsorption study was performed to analyze the equilibrium states, effect of contact time and influence pH value of MSNs (Ebadi and Rafati, 2015). The study was performed with 10 mg adsorbent was added to 5 mL of the solutions with 5 ppm of methylene blue. The solution was stirred for 24 h at 27 °C and 160 RPM to attain equilibrium conditions. Then the samples were centrifugated at 4000 rpm, The residual solution was analyzed using Uv-Vis spectrophotometer at 665 nm. Then adsorption capacity per unit mass (q), was calculated with the following equation (mg/g). where Co (mg/L) is the initial concentration, Ct (mg/L) is the concentration of dye after equilibrium time, V (L) is the volume of solution, and m is the mass of adsorbent.

$$Q = \frac{C_0 - C_t}{m} V \quad (1)$$

2.2.10 Entrapment Efficiency

The MSN-P/GE was separated through centrifugation. The supernatant was collected and analyzed to determine the loaded concentration of *Uncaria gambir* extract and phycocyanin. The collected supernatants were measured with UV-Vis spectrophotometry at 620 nm to determine the concentration of phycocyanin. The supernatants were also measured at 370 nm which indicated the maximum absorption of Quercetin to identify and calculate the concentration of *Uncaria gambir* extract. The entrapment efficiency percentage was calculated using the following equation. Co is concentration of drug fed initially to MSN-P/GE. Ct is concentration of drug in supernatant that

was not encapsulated inside the MSN-P/GE.

$$\text{Entrapment efficiency (\%)} = \frac{C_0 - C_t}{C_t} \times 100 \quad (2)$$

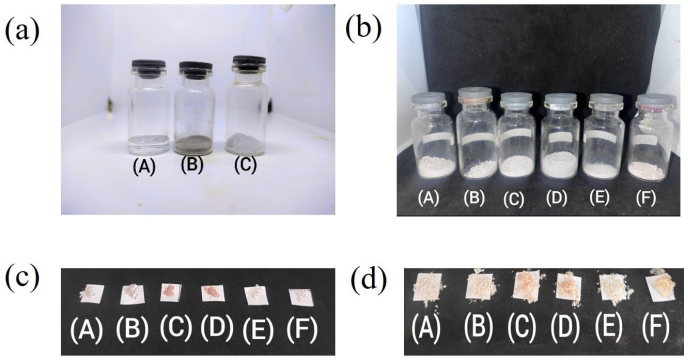

Figure 2. (a) Different Precursor Types Utilized within This Study from L-R: TEOS, Cogon Grass Silica, and Sodium Silicate. (b) Synthesised MSNs with Different Precursor Types and Fabrication Methods, from L-R: TEOS Reflux Method, TEOS Calcination Method, Cogon Grass Reflux Method, Cogon Grass Calcination Method, Sodium Silicate Reflux Method, and Sodium Silicate Calcination Method. (c) Obtained MSNs from (b) Followed by Coating with Chitosan and Gelatine (d)

2.2.11 Photothermal Increase

The photothermal performance of the MSNs@CS-P/GE and MSNs@G-P/GE formulation was evaluated by measuring the temperature increase under visible laser irradiation. A total of 10 mg of MSNs was dispersed in 2.0 mL of deionized water to prepare a 10% (w/v) suspension. The prepared suspension was transferred into a 5 mL transparent glass vial. The sample was irradiated with a 450 nm laser for 300 seconds. The laser beam, operated at a constant power, was directed perpendicularly to the side of the vial. A thermocouple was inserted into the solution to monitor temperature elevation, while ensuring that the laser beam did not directly hit the temperature probe. Temperature measurements were recorded every 10 seconds for a total of 300 seconds. This was conducted to assess the photothermal conversion efficiency of the MSNs formulation (Wang et al., 2020).

2.2.12 In Silico Studies

In silico studies were performed using the bioactive compounds of *Uncaria gambir* extract againts *Staphylococcus aureus* receptor. Ligand and receptor structures were optimized using PyRx - Python Prescription 0.8 (Ayodele et al., 2024; Kannan et al., 2024). The 3D structures of *Uncaria gambir* bioactive compounds were retrieved from PubChem and converted to PDBQT format using Open Babel. Protein structures of *Staphylococcus aureus* (IN67, 2W9G, 4E4R) were obtained from RCSB PDB and refined in Discovery Studio Visualizer by removing water molecules and native ligands, followed by addition of polar hydrogens. Docking was performed using AutoDock Vina via the PyRx interface, with grid boxes set around the original ligand binding sites. Default parameters were applied. Binding free energy (ΔG_binding) results were tabulated and visualized in both 2D and 3D using Discovery Studio Visualizer In silico studies were performed using the bioactive compounds of *Uncaria gambir* extract againts *Staphylococcus aureus* receptor. Ligand and receptor structures were optimized using PyRx - Python Prescription 0.8 (Ayodele et al., 2024; Kannan et al., 2024). The 3D structures of *Uncaria gambir* bioactive compounds were retrieved from PubChem and converted to PDBQT format using Open Babel. Protein structures of *Staphylococcus aureus* (IN67, 2W9G, 4E4R) were obtained from RCSB PDB and refined in Discovery Studio Visualizer by removing water molecules and native ligands, followed by addition of polar hydrogens. Docking was performed using AutoDock Vina via the PyRx interface, with grid boxes set around the original ligand binding sites. Default parameters were applied. Binding free energy (ΔG_binding) results were tabulated and visualized in both 2D and 3D using Discovery Studio Visualizer (Dharsono et al., 2023).

3. RESULT AND DISCUSSIONS

3.1 Characterization of Mesoporous Silica

In this study we explored the effects of 3 factors, namely: precursors type, fabrication method and coating agent (Figure 2). We have successfully extract silica from cogon grass, which is one of the most abundant grass type of plants in the world and easily attainable. This could be an alternative to MSN synthesized from TEOS which is more expensive and sodium silicate which have shown to have low bioavailability and difficult scalability. Due to this limitation, green synthesis of silica from natural sourced materials are excellent alternatives which needs further exploration. Cogon grass mesoporous silica (MSN) has yet to be explored further for drug carrier especially for the antimicrobial treatment.

Adsorption evaluation was carried out with methylene blue to see the uptake by MSN with different precursors. The adsorbing performance was shown in Figure 3(a). The result showed that MSN from cogon grass obtained by calcination gave the best result with 2.179 mg/g uptake for methylene blue under studied conditions (10 mg adsorbent, 5 mg/L, pH 7) and for the reflux (0.415 mg/g). The Cogon grass and TEOS precursors also showed similar results where the calcination method manages to absorb more methylene blue. This result has proof that calcination gave the best results because of the surfactants removal so nothing surfactant left in pores.

Anova analysis showed that the methods factor (calcination and reflux) has very significant influence on mesoporous characterization with p value (p <0.001). Calcination gives the highest porosities, the removal of surfactants, and stable particles structure. In contrast, reflux creates MSN with less purities because of surfactants that have not fully removed. Row factors (precursors) have significant effect based on multiple

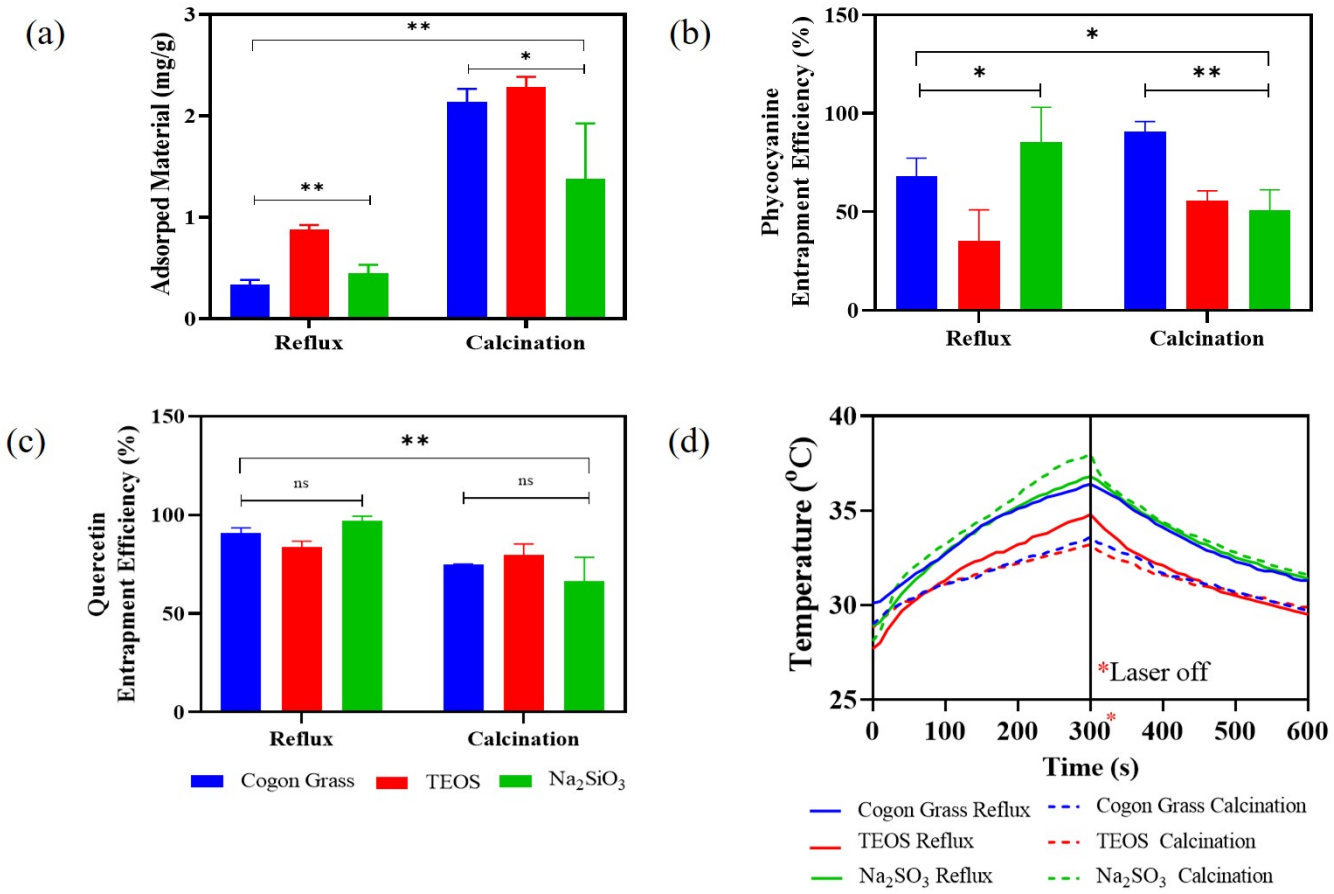

Figure 3. Evaluation of Adsorption on Each Precursor Type and Method (b); Results of Entrapment Efficiency of Phycocyanin (b) and *Uncaria gambir* Extract (c) as Photosensitizers; (d) Photothermal Increase Facilitated by MSN Particles Loaded with Photosensitizer

comparison analysis. TEOS has been proven to be significantly different from sodium silicate or cogon grass. The difference can be explained by the higher purities of TEOS to be synthetic precursors, resulting in more controlled physicochemical properties. Further analysis showed significant interactions between precursors and methods (row × column) with $p < 0.05$. This significant interaction indicates that influence of synthesis methods is not applicable to all precursors. The result showed that the method of synthesis is the dominant factor, but the precursor still contributes in determining the properties of MSN.

MSNs@CS-P/GE has potential in photothermal therapy due phycocyanine capability to convert NIR light energy into photothermal heat. To investigate the photothermal effect, the temperature of the solutions containing different MSNs formulations were measured under laser irradiation (450 nm, 300s). The result of the mesoporous irradiation was shown in Figure 3(c). The result from diagram shown the rapid temperature increase in Sodium Silicate calcination with temperature increase rapidly to 9 °C from 28.5-37.95 °C In 5 minutes. In another method for reflux the temperature increases from 29.8-35.1 °C. These two different methods show that the calcination method has shown the highest increase in temperature, probably due to surfactants that are still there due to temperature removal of surfactants. The temperature for Cogon grass calcination increased from 29.56 °C to 34.5 °C where it increased higher than reflux method which only a little different. For the reflux method the temperature increased from 30.05-35.54 °C. These results are different with TEOS precursors where the reflux method shown significance increase in temperature than calcination. Temperature increased from 28.76-33.2 °C for calcination and for reflux method, the temperature increased from 27.7 °C to 34.76 °C. TEOS as a precursor showed its difference with the last method, where the calcination showed the highest temperature increase than reflux.

Characterization of entrapment efficiency (EE) revealed that both the precursor and the surfactant removal method significantly influenced the drug-loading capacity of the resulting mesoporous materials. In general, the reflux method tended to yield higher EE values for quercetin compared to

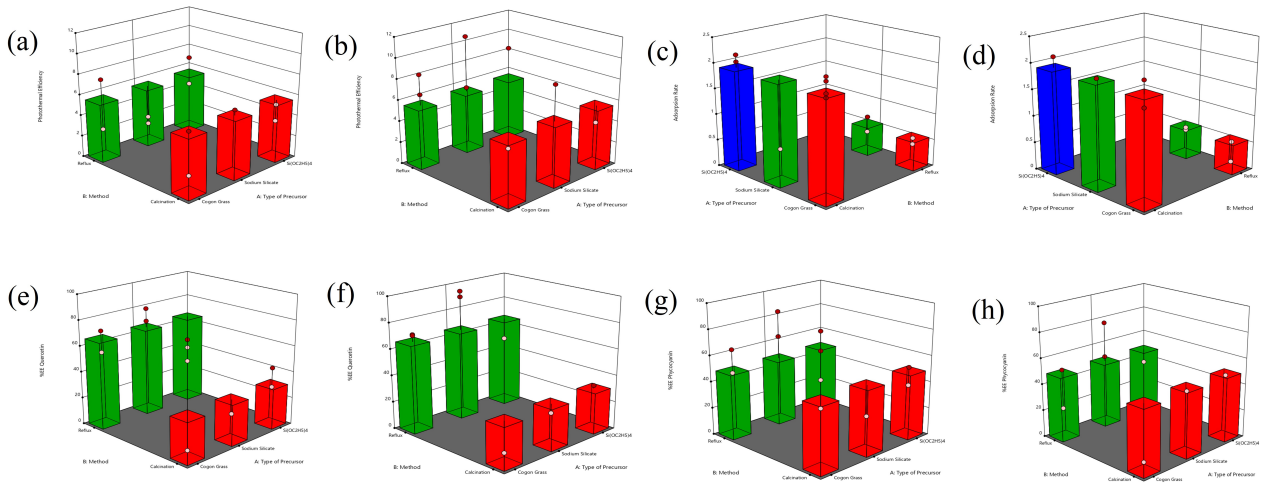

Figure 4. Optimization Results of MSN Synthesis with Different Precursor Types, Fabrication Methods, and Coating Agents. Effect of Precursor Types and Fabrication Methods on Photothermal Increase with Chitosan Coating (a) and Gelatine Coating (b). Difference in Absorption Rate Caused by Precursor Types and Fabrication Methods with Chitosan Coating (c) Compared to Gelatine (d). Effect of Factors Toward Entrapment Efficiency of *Uncaria gambir* Extract Shown in Graphs (e) and (f), While Photosensitizer Entrapment is Shown in (g) and (h)

Table 1. Optimization Results Based on Variation of Three Factors

Run	Precursor Type	Method	Coating Agent	R1	R2	R3	R4
1	Cogon grass	Calcination	CH	1.674	5.907	44.233	2.22
2	TEOS	Calcination	GE	4.060	33.665	48.433	2.135
3	TEOS	Calcination	CH	5.240	29.395	52.476	2.043
4	Cogon grass	Reflux	CH	7.648	72.811	48.100	0.432
5	Cogon grass	Calcination	GE	4.833	8.042	6.766	2.174
6	Cogon grass	Reflux	CH	2.767	56.441	65.766	0.554
7	Na_2SiO_3	Reflux	GE	10.964	92.028	53.100	0.482
8	Na_2SiO_3	Reflux	CH	1.800	81.352	66.766	0.706
9	TEOS	Reflux	CH	4.589	40.782	21.233	0.849
10	Na_2SiO_3	Calcination	CH	6.206	20.318	26.433	0.638
11	Na_2SiO_3	Reflux	CH	2.494	71.622	86.100	0.396
12	Cogon grass	Reflux	GE	8.578	71.387	52.433	0.142
13	TEOS	Reflux	CH	7.334	29.181	62.367	0.940
14	Na_2SiO_3	Reflux	GE	6.048	96.298	79.766	0.532
15	TEOS	Reflux	GE	8.733	50.989	39.100	0.663
16	Cogon grass	Calcination	CH	5.796	84.911	83.766	2.142
17	Na_2SiO_3	Calcination	GE	9.011	24.412	47.100	1.967
18	Cogon grass	Reflux	GE	6.702	72.099	22.433	0.532
19	TEOS	Calcination	CH	3.630	44.341	38.656	2.174

R1: photothermal increase, R2: entrapment efficiency of quercetin, R3: entrapment efficiency of phycocyanin, R4: adsorption rate

the calcination method, whereas its effect on phycocyanin varied depending on the precursor employed. The use of three different precursors-cogon grass, TEOS, and Na_2SiO_3 showed different entrapment efficiency (EE) profiles when applied using calcination method (500 °C, 4 h) and reflux method (80 °C, 24 h). Figure 3(b) and 3(c) shows that for the cogon grass precursor, the EE of Quercetin obtained using the reflux method was higher compared to the calcination method, whereas the EE of Phycocyanin exhibited only a slight difference between the two methods. This indicates that the pore structure pre-

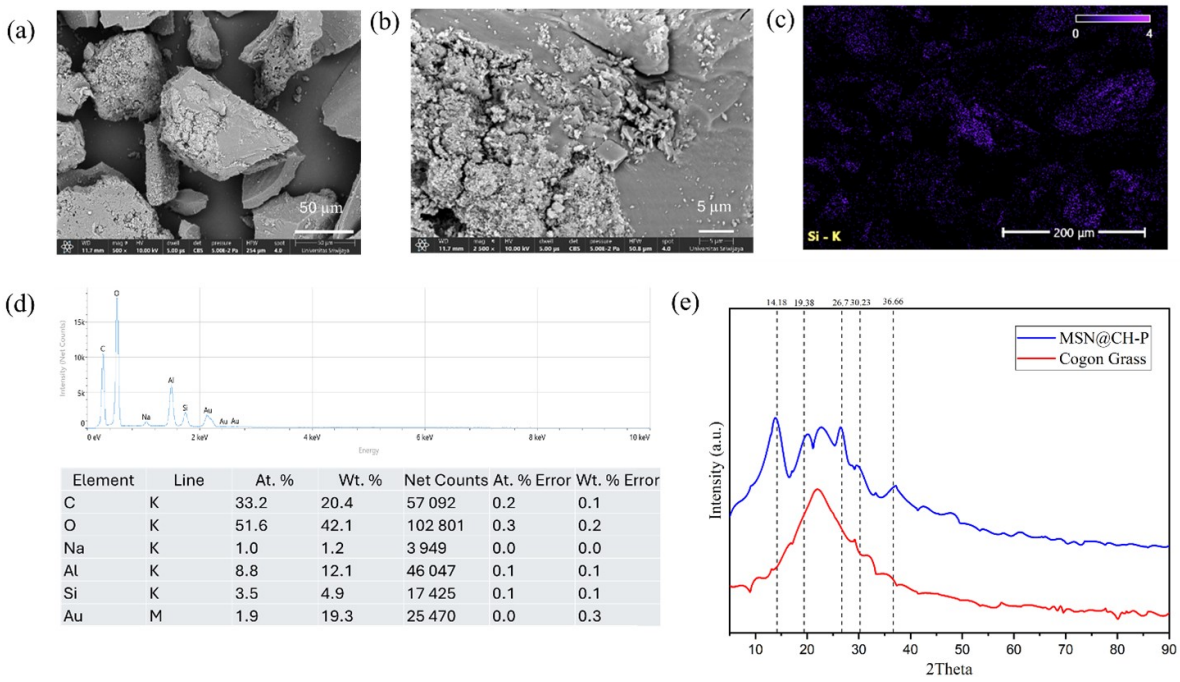

Element	Line	At. %	Wt. %	Net Counts	At. % Error	Wt. % Error
C	K	33.2	20.4	57 092	0.2	0.1
O	K	51.6	42.1	102 801	0.3	0.2
Na	K	1.0	1.2	3 949	0.0	0.0
Al	K	8.8	12.1	46 047	0.1	0.1
Si	K	3.5	4.9	17 425	0.1	0.1
Au	M	1.9	19.3	25 470	0.0	0.3

Figure 5. Results of Optimum Formula Containing MSNs From Cogon Grass with (a) and (b) Displaying the SEM Results at Different Magnifications, and (c, d) Providing Information Regarding the Mapping of Elements Present in the Mixtures. Additionally, XRD Profile (e) Showcasing Amorphous Structure with Presence of Crystalline-Like Structure of the Produced MSNs. (f, d) SEM Histogram Magnified 250× and 500×

Table 2. Binding Energy (Δ*G*) of 18 *Uncaria gambir* Bioactive Compounds Docked Towards Target Proteins in Methicillin Resistant *Staphylococcus aureus*

Bioactive Compound	TLR2	VWF	TNF	PBP2a
(+)-Catechin	-6.4	-5.7	-7.1	-7.7
(-)-Epicatechin	-6.5	-5.9	-8.4	-8.4
(+)-Epicatechin	-6.5	-6.3	-8.4	-8.4
Mitraphylline	-6.8	-6.4	-8.4	-7.7
Roxburghine B	-7.9	-7.8	-10.6	-9.5
Catechol	-5.2	-4.0	-5.7	-5.2
Gallic acid	-6.0	-6.0	-5.7	-6.0
Cinchonain Ia	-9.5	-8.0	-9.3	-8.9
Gambiriin C	-9.3	-8.0	-8.6	-9.6
Gambiriin A1	-9.2	-7.3	-9.5	-9.1
Gambiriin A3	-9.5	-7.5	-8.9	-10.3
Gambiriin B1	-8.7	-7.2	-9.6	-9.3
Gambiriin B3	-9.0	-7.2	-10.0	-9.8
Procyanidin B3	-8.2	-7.0	-9.0	-9.6
Procyanidin B1	-9.0	-8.0	-9.0	-9.6
Ursane B	-8.7	-7.1	-8.0	-7.8
Gambiriin A2	-8.5	-7.0	-9.3	-9.1
Gambiriin B2	-8.6	-7.2	-9.3	-9.4
Vancomycin	-10.8	-7.9	-10.3	-11.2

served through reflux is more favourable for the adsorption of the smaller and more lipophilic quercetin. In contrast, the

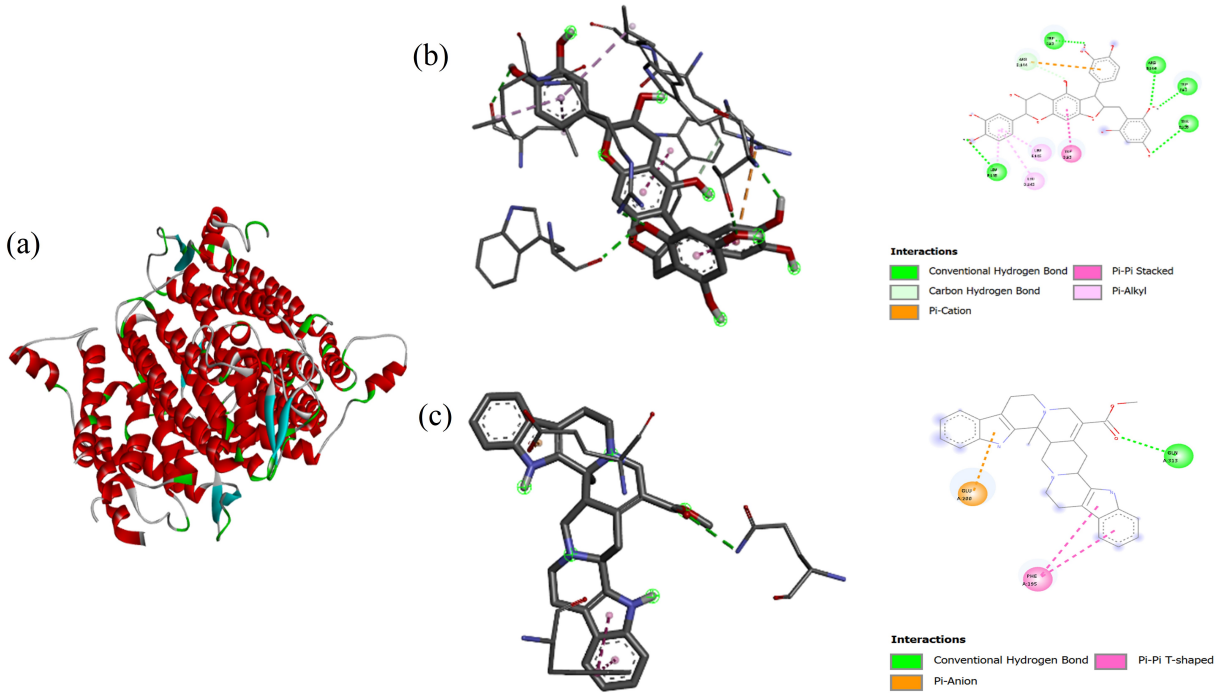

Figure 6. Receptor Specific on MRSA (a) and Their Interactions with Gambiriin (b) and Roxburghin (c)

effect on Phycocyanin is more limited due to its nature as a large hydrophilic protein.

The entrapment efficiency of Quercetin using the TEOS precursor showed a similar trend to that of Quercetin with other precursors, whereas the EE of Phycocyanin under the reflux method was lower compared to the calcination method. The significant differences in EE for both Quercetin and Phycocyanin in the Na_2SiO_3 precursor after reflux indicate that this method produces materials with optimal pore structure and volume for both types of molecules, without experiencing degradation or pore decrease due to high temperatures. In general, these results support the idea that a softer surfactant treatment method (reflux) and the selection of the appropriate precursor are crucial in MSN design to maximize the loading capacity of active molecules, especially for combinations of compounds with different physical properties such as Quercetin and Phycocyanin. No significant differences in entrapment efficiency were observed between precursors (cogon grass, TEOS, Na_2SiO_3) or synthesis methods (calcination, reflux) for either quercetin or phycocyanin (adjusted p >0.05).

Based on the results seen in Table 1 and after evaluation of the effects from each factors optimization was conducted using Design Expert 13 to obtain the best formula. From each response (seen in Table 1 and Figure 4), cogon grass-based MSN were able to produce satisfactory results comparable and even better than sodium silicate and TEOS MSN. From this observation we were able to conclude that silica precursor obtained from cogon-grass is viable to be utilized further for the use antimicrobial purposes.

The most optimum result was followed with further testing including SEM-EDS mapping and XRD analysis. From the SEM result in Figure 5(a) and 5(b), the resulting MSN was porous shown by the irregularity on the surface. However further modification is needed to maximize homogeneity of the presence of these pores to enhance entrapment and adsorption ability of the MSN. EDS mapping further confirmed the presence of silica from cogon grass MSN (Figure 5c) with 4.6% percentage in mass as shown in Figure 5(d). Based on the XRD result (Figure 5e), cogon-grass MSN was amorphous with more crystalline formation occurring, due to the addition of CTAB and calcination or reflux during the fabrication process.

Prior to evaluation of antimicrobial effect on an invitro antibacterial model, we conducted in silico evaluation of *Uncaria gambir* as antimicrobial towards MRSA with activity towards TLR2, VWF, TNF and PBP2a as the most common receptors in MRSA. Results in Table 2 indicated that compounds such as Gambiriin, Roxburghine and Procyanidin produced the highest effect towards the receptors. Additional evaluation towards *Staphylococcus aureus* showed that the compounds work more effective on target proteins ClfA and DHFR with maximum binding energy values of respectively -10.4 and -10.5 kcal/mol (Table 3). From the three receptors, Roxburghine B appears to have a prominent contribution as Methicillin resistant *S. aureus* inhibitor, shown by the high binding score in ClfA, DHFR and the highest in Pta. Gambiriin A1, Gambiriin A2, and Roxburghine B hold the best binding affinity towards ClfA. Both Procyanidine B3 and Roxburghine B are recorded to have huge tendency to inhibit the synthesis of DHFR, fol-

Table 3. Binding Energy (ΔG) of 18 *Uncaria gambir* Bioactive Compounds Docked Towards Target Proteins in *Staphylococcus aureus*

Bioactive Compound	ΔG Binding (kcal/mol)		
	Clumping factor A (1N67)	Dihydrofolate Reductase (2W9G)	Phosphotransacetylase (4E4R)
(−)-Epicatechin	-8.2	-8.6	-7.6
(+)-Cathechin	-8.2	-8.7	-7.6
(+)-Epicatechin	-8.2	-8.7	-7.6
Catechol	-5.0	-4.9	-5.1
Cinchonain Ia	-9.5	-10.3	-7.7
Gallic Acid	-6.6	-5.7	-6.9
Gambiriin A1	-10.4	-9.1	-8.4
Gambiriin A2	-10.4	-9.2	-8.4
Gambiriin A3	-9.1	-8.1	-8.8
Gambiriin B1	-9.3	-9.9	-8.0
Gambiriin B2	-9.3	-9.0	-8.0
Gambiriin B3	-9.5	-9.6	-8.4
Gambiriin C	-9.6	-7.7	-7.8
Mitraphylline	-9.3	-8.7	-6.7
Procyanidin B1	-9.4	-9.5	-8.8
Procyanidin B3	-9.3	-10.5	-8.8
Roxburghine B	-10.1	-10.5	-9.7
Uncarine B	-8.1	-6.8	-6.9

lowed by Cinchonain Ia and Pta, followed by Gambiriin A1 and Procyanidin B1.

The second most promising compound, Roxburghine B were able to form three hydrogen bonds with DHFR (SER49, GLN19, LEU20), a hydrophobic pi-alkyl bond (ILE14), and a pi-sigma bond (LEU28), meanwhile hydrophilic bonds are not observed when docked with Pta. Procyanidin B3 interacts with DHFR through five hydrogen bonds (SER49, LEU28, THR46, ASN18, LYS45), pi-alkyl bonds (ILE50, LEU54, VAL31), and unfavorable donor-donor (LEU20, LYS32). Gambiriin A1 and Gambiriin A2 possess similar binding activities with ClfA namely hydrogen, unfavorable donor-donor, pi-cation, pi-pi T-shaped, and pi-alkyl bonds. These interactions from Gambiriin and Roxburghin with the MRSA receptor can be seen in Figure 6(a-c). Based on these findings we were able to demonstrate strong potential of *Uncaria gambir* extract to be utilised for MRSA and their incorporation into a carrier MSN-based system from cogon-grass.

4. CONCLUSIONS

In summary, we have successfully extracted silica from cogon grass and utilized it for the synthesis of mesoporous silica nanoparticle with quality comparable to the widely used precursors TEOS and sodium silicate. These findings indicate the strong potential of cogon-grass based MSN to be further developed in the future as drug delivery carrier. Furthermore, we have shown successful loading of phytocompounds including photosensitizers which demonstrate the ability of the MSN in enhancing photothermal increase. In addition, we have also confirmed our hypothesis towards *Uncaria gambir* activity as anti-MRSA therapy on an in-silico model. This result will be the foundation of further research into the invitro and invivo application of *Uncaria gambir* in AMR management.

5. ACKNOWLEDGEMENT

Authors would like to express gratitude towards Direktorat Penelitian dan Pengabdian Kepada Masyarakat Direktorat Jenderal Riset dan Pengembangan Kementerian Pendidikan Tinggi, Sains dan Teknologi Sesuai Kontrak Pelaksanaan Program Bantuan Operasional Perguruan Tinggi Negeri Program Penelitian No. 109/C3/DT.05.00/PL/2025 for providing the financial support used within this study.

REFERENCES

Abbasianfar, Z., B. Seraj, S. Afrasiabi, M. J. K. Fard, S. Ghadimi, and N. Chiniforush (2024). The Effect of Antimicrobial Photodynamic Therapy Using Different Concentrations of Phycocyanin against Streptococcus Mutans. *Photodiagnosis and Photodynamic Therapy*, **50**; 104384

Ahmed, S. K., S. Hussein, K. Qurbani, R. H. Ibrahim, A. Fareeq, K. A. Mahmood, and M. G. Mohamed (2024). Antimicrobial Resistance: Impacts, Challenges, and Future Prospects. *Journal of Medicine, Surgery, and Public Health*, **2**; 100081

Ayodele, O. A., I. O. Awotuya, B. J. Taiwo, O. M. Osungunna, M. Vuyisa, and S. L. Kasim (2024). Two New Triterpenoids from the Leaf of *Ficus vogelii* and Their Antibacterial Activities. *Chemistry Africa*, **7**(1); 63–70

Azzahra, F. D., L. N. Mulyani, T. Sabrina, and N. A. Fithri (2025). Liposome Photosensitizer with Enzyme from Black Soybean Tempeh: Formula Optimization and In Vitro Thrombolytic Activity Evaluation. *Science and Technology Indonesia*, **10**(3); 903–915

Chen, F. and Y. Zhu (2012). Chitosan Enclosed Mesoporous Silica Nanoparticles As Drug Nano-Carriers: Sensitive Response to the Narrow pH Range. *Microporous and Mesoporous Materials*, **150**; 83–89

Cieplik, F., D. Deng, W. Crielaard, W. Buchalla, E. Hellwig, A. Al-Ahmad, and T. Maisch (2018). Antimicrobial Photodynamic Therapy–What We Know and What We Don't. *Critical Reviews in Microbiology*, **44**(5); 571–589

Dharsono, H. D. A., M. Mujahid, E. Apriyanti, R. A. F. Adang, S. A. Putri, M. H. Satari, and D. Kurnia (2023). Tannin Derived from *Uncaria gambir* Roxb. As Potential Enterococcus Faecalis UDP-N-Acetylenolpyruvoyl-glucosamine Reductase (Mur Benzyme) Inhibitor: In-Silico Antibacterial Study. *Research Journal of Pharmacy and Technology*, **16**(10); 4568–4574

Dorairaj, D., N. Govender, S. Zakaria, and R. Wickneswari (2022). Green Synthesis and Characterization of UKMRC-8 Rice Husk-Derived Mesoporous Silica Nanoparticle for Agricultural Application. *Scientific Reports*, **12**(1); 20162

Ebadi, A. and A. A. Rafati (2015). Preparation of Silica Mesoporous Nanoparticles Functionalized with β-Cyclodextrin and Its Application for Methylene Blue Removal. *Journal of Molecular Liquids*, **209**; 239–245

Fithri, N. A., A. Fadilah, A. Pratiwi, S. S. Alisyahbana, M. F. Alhafiz, N. P. Maharani, et al. (2025). *Uncaria gambir* Based Green Synthesis of Inorganic Nanoparticles for Photothermal Induced Thrombolytic and Antibacterial Applications. *Science and Technology Indonesia*, **10**(1); 303–312

Han, Y., L. Zhang, and W. Yang (2024). Synthesis of Mesoporous Silica Using the Sol–Gel Approach: Adjusting Architecture and Composition for Novel Applications. *Nanomaterials*, **14**(11); 903

Ho, C. S., C. T. Wong, T. T. Aung, R. Lakshminarayanan, J. S. Mehta, S. Rauz, A. McNally, B. Kintses, S. J. Peacock, C. de la Fuente-Nunez, et al. (2025). Antimicrobial Resistance: A Concise Update. *The Lancet Microbe*, **6**(1); 1–14

Ikuta, K. S., L. R. Swetschinski, G. R. Aguilar, F. Sharara, T. Mestrovic, A. P. Gray, N. D. Weaver, E. E. Wool, C. Han, and A. G. Hayoon (2022). Global Mortality Associated with 33 Bacterial Pathogens in 2019: A Systematic Analysis for the Global Burden of Disease Study 2019. *The Lancet*, **400**(10369); 2221–2248

Kannan, C., M. Radhakrishnan, D. Sambathkumar, M. Dhanaraja, M. Muvendhiran, and M. Dharnisha (2024). A Review on Step into the Future: Python Prescription (PyRx) Transforms Virtual Drug Discovery with AI-Driven Tools. *African Journal of Biomedical Research*, **27**(3S); 790–795

Krishnan, V., M. Suresh, T. Kalaivani, et al. (2022). Synthesis and Characterization of Mesoporous SiO_2 Nanoparticles for Bio Medical Applications. In *IOP Conference Series: Materials Science and Engineering*, volume 1219. IOP Publishing, page 012038

Liu, J., L. Zhang, H. Ma, H. Sun, S.-a. Ge, J. Liu, S. Fan, and C. Quan (2025). Quaternary Ammonium Chitosan-Functionalized Mesoporous Silica Nanoparticles: A Promising Targeted Drug Delivery System for the Treatment of Intracellular MRSA Infection. *Carbohydrate Polymers*, **352**; 123184

Mardiyanto, M., I. Sholihah, and T. G. Jaya (2020). The Chitosan-Sodium Alginate Submicro Particles Loading Herbal of Ethanolic Exract of Leaves *Senna alata.* L for Curing of Bacterial Infection on Skin. *Science and Technology Indonesia*, **5**(3); 85–89

Naghavi, M., S. E. Vollset, K. S. Ikuta, L. R. Swetschinski, A. P. Gray, E. E. Wool, G. R. Aguilar, T. Mestrovic, G. Smith, and C. Han (2024). Global Burden of Bacterial Antimicrobial Resistance 1990–2021: A Systematic Analysis with Forecasts to 2050. *The Lancet*, **404**(10459); 1199–1226

Narayan, R., U. Y. Nayak, A. M. Raichur, and S. Garg (2018). Mesoporous Silica Nanoparticles: A Comprehensive Review on Synthesis and Recent Advances. *Pharmaceutics*, **10**(3); 118

Nasab, N. A., H. H. Kumleh, M. Beygzadeh, S. Teimourian, and M. Kazemzad (2018). Delivery of Curcumin by a pH-Responsive Chitosan Mesoporous Silica Nanoparticles for Cancer Treatment. *Artificial Cells, Nanomedicine, and Biotechnology*, **46**(1); 75–81

Overchuk, M., R. A. Weersink, B. C. Wilson, and G. Zheng (2023). Photodynamic and Photothermal Therapies: Synergy Opportunities for Nanomedicine. *ACS Nano*, **17**(9); 7979–8003

Putz, A.-M., S. Cecilia, C. Ianăşi, Z. Dudás, K. N. Szekely, J. Plocek, P. Sfârloagă, L. Săcărescu, and L. Almasy (2015). Pore Ordering in Mesoporous Matrices Induced by Different Directing Agents. *Journal of Porous Materials*, **22**(2); 321–331

Rahmat, N., F. Hamzah, N. Sahiron, M. Mazlan, and M. M. Zahari (2016). Sodium Silicate As Source of Silica for Synthesis of Mesoporous SBA-15. In *IOP Conference Series: Materials Science and Engineering*, volume 133. IOP Publishing, page 012011

Singha, B., V. Singh, and V. Soni (2024). Alternative Therapeutics to Control Antimicrobial Resistance: A General Perspective. *Frontiers in Drug Discovery*, **4**; 1385460

Usgodaarachchi, L., C. Thambiliyagodage, R. Wijesekera, and M. G. Bakker (2021). Synthesis of Mesoporous Silica Nanoparticles Derived from Rice Husk and Surface-Controlled Amine Functionalization for Efficient Adsorption of Methylene Blue from Aqueous Solution. *Current Research in Green and Sustainable Chemistry*, **4**; 100116

Vallet-Regí, M., F. Schüth, D. Lozano, M. Colilla, and M. Manzano (2022). Engineering Mesoporous Silica Nanoparticles

for Drug Delivery: Where Are We After Two Decades? *Chemical Society Reviews*, **51**(13); 5365–5451

Varala, R., V. Kotra, A. K. Kanuri, M. R. Burra, and S. Nyamathullah (2023). Nano Drug Delivery-benefits, Limitations and Future Perspective. *Nano and Medical Materials*, **3**(1); 244–244

Wang, Y., C. Niu, S. Fan, Y. Li, X. Li, Y. Dai, J. Shi, and X. Wang (2020). Indocyanine Green Loaded Modified Mesoporous Silica Nanoparticles As an Effective Photothermal Nanoplatform. *International Journal of Molecular Sciences*, **21**(13); 4789

Zhang, M., C. Xu, L. Wen, M. K. Han, B. Xiao, J. Zhou, Y. Zhang, Z. Zhang, E. Viennois, and D. Merlin (2016). A Hyaluronidase-Responsive Nanoparticle-Based Drug Delivery System for Targeting Colon Cancer Cells. *Cancer Research*, **76**(24); 7208–7218

Zhu, L., W. Zhang, P. Song, W. Li, X. Chen, F. Ge, L. Gui, K. Yang, Y. Tao, and D. Guocheng (2022). Redox-Responsive Mesoporous Silica Nanoparticles for Chemo-Photodynamic Combination Cancer Therapy. *Materials Research Express*, **9**(4); 045401

